European Journal of Medicinal Chemistry 80 (2014) 1–7

Contents lists available at ScienceDirect

European Journal of Medicinal Chemistry

journal homepage: http://www.elsevier.com/locate/ejmech

Original article

Synthesis, cytotoxicity for mimics of catalase: Inhibitors of lactate dehydrogenase and hypoxia inducible factor

Juan-Juan Xue [a], Qiu-Yun Chen [a,*], Meng-Yun Kong [a], Chun-Yin Zhu [a], Zhi-Rong Gen [b], Zhi-Lin Wang [b]

[a] School of Chemistry and Chemical Engineering, Jiangsu University, Zhenjiang 212013, PR China
[b] State Key Laboratory of Coordination Chemistry, Nanjing University, Nanjing 210093, PR China

ARTICLE INFO

Article history:
Received 31 October 2013
Received in revised form
12 March 2014
Accepted 10 April 2014
Available online 13 April 2014

Keywords:
Mimics of catalase
Cancer cells
LDH
HIF
Manganese

ABSTRACT

Lactate dehydrogenase A (LDH-A) is a potentially important metabolic target for the inhibition of the highly activated glycolysis pathway in cancer cells. Two Mn(II) complexes with ligand containing di(pyridylmethyl) amine and pyrrol-ketone were used to attenuate the activity of LDH-A. The inhibition of the manganese(II) complexes on the proliferation of HepG-2 cells is related to their ability to disproportionate H_2O_2. Importantly, the synthesized mimic of catalase can decrease the expression of hypoxia inducible factor (HIF-1α) in HepG-2 cells. So we envision that the multifunctional mimics of catalase could attenuate the activity of LDH-A signaling the cancer cells to death through HIF-1α involved path.

1. Introduction

Cancer cells typically display altered glucose metabolism characterized by a preference of aerobic glycolysis, known as the Warburg effect, which facilitates cell proliferation [1]. Glycolysis allows for continued ATP production without the need of O_2-dependent oxidative phosphorylation, and is thus an important pathway under hypoxic conditions [2]. Altered cancer cell energy metabolism has been categorized as an emerging hallmark of cancer, and thus, inhibition of metabolic processes associated with cancer cell growth constitutes a promising approach in the search for new cancer therapies [3,4]. One molecular target in the glycolytic pathway is the lactate dehydrogenase (LDH) which catalyzes the interconversion of lactate and pyruvate [5,6]. In mammalian cells, there are four major isoforms of LDH, LDH-A, LDH-b, LDH-c and LDH-h, with the A form having higher intrinsic activity to catalyze the transformation of pyruvate to lactate. LDH-A is a potentially important metabolic target for inhibition of the highly activated glycolysis pathway in cancer cells [7]. Most reported LDH-A inhibitors, such as oxamate, 3-hydroxyisoxazole-4-carboxylic acid and N-hydroxyindole, are competitive with the pyruvate or NADH substrate binding [7–9]. Moreover, targeted inhibition of HIF-1α is another new pathway to cancer therapy. Hypoxia-inducible factor (HIF-1α) regulates the energy metabolism by triggering a switch from mitochondrial oxidative phosphorylation to anaerobic glycolysis, increasing the expression of genes that encode glycolytic enzymes and glucose transporters [10]. Cancer cells activate glycolysis to meet their energy demands and use O_2 to generate excessive levels of the reactive oxygen species (ROS), superoxide anion ($O_2^{\cdot-}$) and hydrogen peroxide (H_2O_2). H_2O_2, a kind of ROS generated in mitochondria, is considered a mediator of apoptotic cancer cell, and can be eliminated by mitochondrial catalase [11,12]. With the over-expression of H_2O_2-detoxifying enzymes or human catalase *in vivo*, H_2O_2 concentration will decrease, and cancer cells could revert to normal appearance [13]. Thus, H_2O_2 is also an important signal molecule to attenuate the metabolite of oxygen in cancer cells and the catalase could be a modulator of HIF-1α signals.

It is reported that the manganese(III) porphyrin complexes could decrease the mitochondrial H_2O_2 [14]. Previously we found that the carboxylate-bridged dimanganese(II) systems could be used as functional models of catalase, which could inhibit the

Abbreviations: LDH-A, Lactate dehydrogenase; HIF, hypoxia inducible factor; dpa, Di(pyridine-2-yl)methyl)amine; PPMdpa, 4-(Chloromethyl)phenyl)(3,5-dimethyl-1*H*-pyrrol-2-yl)methanone); pydpa, *N*-(3-Pyridyl)methyl-di(pyridylmethyl)amine; phdpa, *N*-Benzyl-di(pyridylmethyl)amine; Mn1, [(PPMdpa)$MnCl_2$]; Mn2, [(PPMdpa)$MnAc_2$]; Hepes, 4-(2-Hydroxyethyl)-1-pierazineethanesulfonic acid; DMEM, Dulbecoo's modified Eagle's medium.

* Corresponding author.
E-mail address: chenqy@ujs.edu.cn (Q.-Y. Chen).

http://dx.doi.org/10.1016/j.ejmech.2014.04.035
0223-5234/

proliferation of HeLa cells through ROS signal induced apoptosis [15]. These lipophilic complexes can accumulate in cancer cells through perturbing the mitochondrial membrane potential or inhibiting the swelling of over calcium(II) loaded mitochondria [16,17]. Thus, we propose that the conjugation of pyrrol-conjugated C═O groups (3,5-dimethyl-1H-pyrrole-2-carbonyl portion, Scheme 1 and Scheme S1) with Mn(II) complexes of di(picolyl) amine would produce a new kind of multifunctional complexes with activity of inhibiting LDH-A and HIF-1α. Here, we report the synthesis, characterization and bioactivities of Mn(II) complexes of PPMdpa.

2. Results and discussion

2.1. Synthesis and characterization of ligand (PPMdpa) and complexes

Di(pyridine-2-ylmethyl)amine (dpa) and 4-(chloromethyl) phenyl)(3,5-dimethyl-1H-pyrrol-2-yl)methanone (PPM) were refluxed in acetonitrile under nitrogen producing PPMdpa in 66% yield (Scheme S1). The ^{1}H NMR spectra of the PPM and PPMdpa confirm the existence of PPMdpa (Figs. S1 and S2). Subsequent reaction of PPMdpa with $MnCl_2{\cdot}4H_2O$ or $MnAc_2{\cdot}6H_2O$ resulted in the formation of complexes Mn1 or Mn2. The structures of complexes Mn1 and Mn2 were characterized by elemental analyses, IR, UV, ES-MS and EPR. The elemental analyses show that the ratio of metal:L in all complexes is 1:1. The PPMdpa and Mn1 are unsoluble in water, while Mn2 is slightly soluble in water. The δ(CH) vibration of pyridyl ring is at approximately 760 cm^{-1} [18]. In contrast, these vibrations in the complexes Mn1 and Mn2 are all shifted to 762 and 765 cm^{-1}, respectively. These shifts can be explained by the fact that the nitrogen atoms of pyridyl ring of the ligands donate a pair of electrons each to the central metal ions, forming coordinate covalent bond [19]. The ν(C═O) bands of the complexes Mn1 and Mn2 appear at approximately 1610 cm^{-1} and 1606 cm^{-1}, respectively, indicating the existence of the pyrrol-conjugated carbonyl group in PPMdpa (Fig. S3) [20]. The strong peak at 3237 cm^{-1} for Mn1 and Mn2 in infrared spectra was assigned to ν(N–H) stretching frequencies showing the existence of pyrrole in PPMdpa. The stretching frequencies of ν (COO^-) at 1570 cm^{-1} and 1016 cm^{-1} for complex Mn2, indicates the existence of COO^- [21].

The UV spectra of PPMdpa had bands at 206, 248 and 323 nm (Fig. S4 and Table S1). The band at 248 nm can be attributed to the n–π* transition of the pyrrole-conjugated C═O. This band for complexes Mn1 and Mn2 was red shift to 257 nm and 256 nm, respectively. Nearly no free Mn(II) ions could be measured for the solution of Mn1 and Mn2 in water-DMSO (1:1) by ICP methods, indicating Mn1 and Mn2 are stable in solution. The main peak for PPMdpa m/z = 411.36(100) corresponds to species $[(PPMdpa)H]^+$ indicating that the PPMdpa is stable in the ES-MS condition (Fig. S5). The main peak for Mn2 at m/z = 524.29 (100) corresponds to species $[(PPMdpa)Mn(\mu\text{-}Ac)_2Mn(PPMdpa)]^{2+}$, which indicates the existence of Mn2 (Fig. S6). The 50.58% weight loss in the range of 109–540 °C corresponds to the loss of di(pyridylmethyl)amine groups from the ligand and two chlorine ions in Mn1 (calcd 50.37%) (Fig. S7A). Thermal analysis (TG) curves of Mn2 in the range of temperature from 0 to 1000 °C are shown in Fig. S7B. The weight loss of 54.25% at 98–460 °C for Mn2 is attributed to the loss of four Ac^- ions and two dpa groups from the ligand (calcd 54.37%). Thermal analysis results confirm the formation of $[(PPMdpa)Mn(\mu\text{-}Ac)_2Mn(PPMdpa)Ac_2]$ (Mn2). The paramagnetic resonance of the powder solid state complex Mn2 was carried out at 110 K. The EPR spectrum recorded for the Mn2 displays a strong signal centered at g = 2.01 with no hyperfine splitting indicating no Mn–Mn coupling interaction in Mn2, which is consistent with that of those reported dimanganese(II) species (Fig. S8) [22].

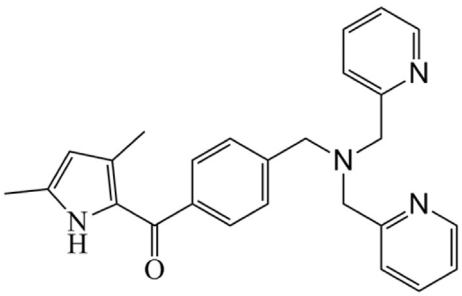

PPMdpa

Scheme 1. The chemical structure of PPMdpa.

2.2. Crystal structure of $[(PPMdpa)_2Mn_2(\mu\text{-}Cl)_2Cl_2]_2$ (Mn1)

The molecular structure of $[(PPMdpa)_2Mn_2(\mu\text{-}Cl)_2Cl_2]_2$ (Mn1) with the atomic labeling scheme is shown Fig. 1, and the selected bond lengths and angles are listed in Table S3. The Mn1 atom in $[(PPMdpa)_2Mn_2(\mu\text{-}Cl)_2Cl_2]_2$ (Mn1) is coordinated by three N atoms (N2, N3, N4), one chloride atom (Cl1), and two bridged chloride anions (Cl2, Cl2A), resulting in a six coordinate dinuclear Mn(II) complex. The complex $[(PPMdpa)_2Mn_2(\mu\text{-}Cl)_2Cl_2]_2$ thus shows a distorted octahedral geometry. Atoms N2, N3, Cl2 and Cl2A form the equatorial tetragonal plane (mean deviation = 0.0828), while N4 and Cl1 occupy the apical positions. The Mn1 atom is shifted by 0.3419 Å out of the equatorial plane toward Cl2. The Mn1–N4 and Mn1–Cl1 bond distances are 2.387(3) and 2.4257(13) Å, respectively. The N4–Mn1–Cl1 angle is 159.28(9) Å. Atoms N2A, N3A, Cl2 and Cl2A form the equatorial tetragonal plane (mean deviation = 0.0828), while N4A and Cl1A occupy the apical positions. The Mn1A atom is shifted by 0.3419 Å out of the equatorial plane toward Cl2. The Mn1–N4 and Mn1–Cl1 bond distances are 2.387(3) and 2.4257(13) Å, respectively. The N4–Mn1–Cl1 angle is 159.28(9) Å.

2.3. Catalase-like activity measured by O_2 evolution – kinetics studies

The progresses of the reactions between complexes and H_2O_2 at various conditions were monitored by UV–vis spectroscopy. When H_2O_2 (0.5 mL, 30%) was added to the white-yellow solution of Mn2, the color of the solution became dark-yellow and poorly resolved absorption bands in the range of 400–800 nm appeared, which indicate that complex Mn2 could bind with H_2O_2 (Fig. S9). The O_2 evolution volume was used for the kinetic study of H_2O_2 disproportionation. The H_2O_2 disproportionation promoted by complexes was carried out in MeCN and buffered solutions ((Tris/Tris–HCl 0.1 M, NaCl 0.1 M, pH 7.4) at 0 and 37 °C. It was found that less gas evolution could be monitored when Mn1 was incubated with H_2O_2, even after 3 h under the conditions described above, demonstrating that Mn1 could not catalyze the disproportionation of dihydrogen peroxide (Fig. 2a). In contrast, complex Mn2 can disproportionate dihydrogen peroxide to generate dioxygen. The complex Mn2 could disproportionate 0.5 mL H_2O_2 aqueous to liberate 1 mmol O_2. The obtained plot of the initial rate vs the concentration of dihydrogen peroxide is fitted by using the Hill equation ($V_0 = V_{max}\ [s]^n/(K_m + [s]^n)$) (Fig. S10, Fig. S11). The parameter K_{cat} is calculated from the equation $K_{cat} = V_{max}/[E_t]$ [23,24]. The maximum O_2 evolution rates were about 4.74 mM s^{-1} and 0.94 mM s^{-1} for Mn2 in the MeCN and Tris–HCl solution, respectively. The Hill constants (n)